Steel and Composite Structures, *Vol. 33, No. 3* (*2019*) *357-373*
DOI: https://doi.org/10.12989/scs.2019.33.3.357

Flexural behavior of steel storage rack base-plate upright connections with concentric anchor bolts

Xianzhong Zhao*[1,2], Zhaoqi Huang [1], Yue Wang [1] and Ken S. Sivakumaran [3]

[1] *Department of Structural Engineering, Tongji University, 1239 Siping Road, Shanghai, 200092, China*
[2] *State Key Laboratory of Disaster Reduction in Civil Engineering, Tongji University, 1239 Siping Road, Shanghai, 200092, China*
[3] *Department of Civil Engineering, McMaster University, Hamilton, Ontario, L8S 4L7, Canada*

(*Received June 1, 2018, Revised October 25, 2019, Accepted October 29, 2019*)

Abstract. Steel storage racks are slender structures whose overall behavior and the capacity depend largely on the flexural behavior of the base-plate to upright connections and on the behavior of beam-to-column connections. The base-plate upright connection assembly details, anchor bolt position in particular, associated with the high-rise steel storage racks differ from those of normal height steel storage racks. Since flexural behavior of high-rise rack base connection is hitherto unavailable, this investigation experimentally establishes the flexural behavior of base-plate upright connections of high-rise steel storage racks. This investigation used an enhanced test setup and considered nine groups of three identical tests to investigate the influence of factors such as axial load, base plate thickness, anchor bolt size, bracket length, and upright thickness. The test observations show that the base-plate assembly may significantly influence the overall behavior of such connections. A rigid plate analytical model and an elastic plate analytical model for the overall rotations stiffness of base-plate upright connections with concentric anchor bolts were constructed, and were found to give better predictions of the initial stiffness of such connections. Analytical model based parametric studies highlight and quantify the interplay of components and provide a means for efficient maximization of overall rotational stiffness of concentrically anchor bolted high-rise rack base-plate upright connections.

Keywords: steel storage racks; base connections; concentric anchor bolts; flexural behavior; experimental; initial stiffness; moment capacity; component method; analytical models for the base plate; parametric study

1. Introduction

Steel pallet rack structural systems are wildly utilized for bulk storage of goods in many business enterprises, such as manufacturing industry, warehouses, retail stores, etc., since such rack structures are easy to construct indoor, and the goods can be easily stored and accessed. The primary structural members of a pallet rack system consist of upright (columns), beams, beam-to-upright connections and column bases. Regular steel pallet racks may be about 10 meters in height, and thus could be an unbraced frame along the down-aisle direction (bay direction). Modern high capacity manufacturing industries, and other similar business enterprises, demand high intensity storage capacities with lower warehouse foot-prints, which essentially requires high-rise storage racks. As a result, the height of modern steel storage racks may be in the range of 20-30 m. Such a tall steel frame structure requires additional stiffening along the down-aisle direction, and thus is usually braced in both directions. Fig. 1 illustrates the configuration and the structural elements associated with a braced high-rise steel storage rack system.

Since, such steel pallet racks are fabricated with thin-walled perforated members, in general, the flexibility of the perforated uprights and beams, as well as the flexibility of the connections, govern the stability and strength of the such rack structures (Silvestre and Camotim 2004, Kadi and Kiymaz 2015). Shah *et al.* (2016) provided a state-of-the-art review on the design and performance of steel pallet rack connections. Correct design and analysis of rack systems must incorporate the semi-rigid nature of the connections (Bernuzzi *et al.* 2015, Valipour and Bradford 2013). Seismic performance of such flexibly connected rack structures is also of great interest due to collapse of such rack structures in recent earthquakes (El Kadi *et al.* 2017,

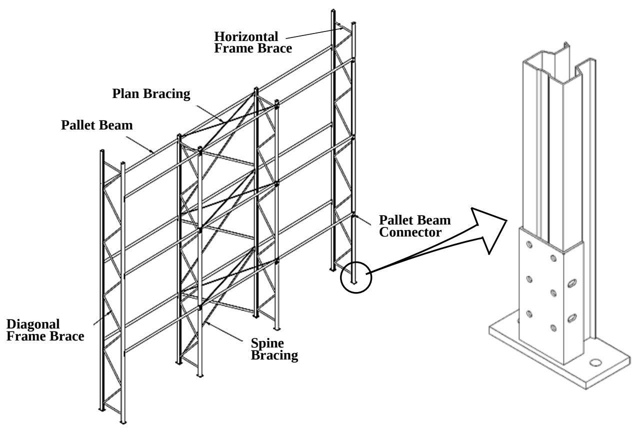

Fig. 1 Elements of a braced high-rise rack structure

*Corresponding author, Ph.D., Professor,
E-mail: x.zhao@tongji.edu.cn

ISSN: 1229-9367 (Print), 1598-6233 (Online)

Kilar *et al.* 2011, Petrone *et al.* 2016, Jacobsen and Tremblay 2017).

At the ground level, the upright is supported on the floor through a base-plate. The column bases of a pallet rack system, namely base-plate upright connection assembly, can influence the lateral stiffness, load carrying capacity and the stability of the pallet rack structure (Baldassino and Bernuzzi 2000, Beale and Godley 2001). Depending on the column base design, the base-plate upright connection assembly may consist one or more of the interlinking components such as upright, bracket, base plate, anchor bolt and the concrete floor. In the very simplest case, the upright end may be just welded to a base plate (foot plate) and the whole pallet rack system simply rests on the floor. Regular pallet racks, made by assembling together beams and uprights (columns) to form an unbraced frame, may have adequate strength, stiffness and stability, even when the upright is not connected to the concrete floor. For the high-rise pallet rack base-plate upright connection assembly, however, a steel bracket is welded to the base plate which is first mounted to the concrete floor using anchor bolts, and then the upright is fastened to the bracket using connecting bolts. The resulting base-plate upright connection for high-rise storage racks is highlighted in Fig. 1. Furthermore, compared with regular unbraced pallet racks, the high-rise braced pallet racks may require base-plate upright connections possessing higher flexural stiffness and higher moment capacities. Improved structural characteristics may be achieved by (a) providing thicker base plates than those used in regular pallet racks, and (b) by changing the anchor bolt locations. The objectives of this investigation are to experimentally investigate the initial rotational stiffness and moment capacity of concentrically anchor bolted base-plate upright connections for high-rise pallet racks, and to establish analytical methodologies in order to quantify such structural parameters.

An engineer interested in high-rise steel storage rack design may consult existing specifications in order to obtain the initial stiffness and the moment capacity of the base-plate upright connections. The widely used specifications for pallet rack design (i.e., Specification for the design, testing and utilization of industrial steel storage racks (RMI 2008), Steel static storage systems—adjustable pallet racking systems—principles for structural design, EN 15512 (CEN 2009) and AS/NZS 4084- Steel storage racking (SA 2012)) propose different approaches to determine the initial stiffness of the base-plate upright connection assemblies. The RMI (2008) specification proposes an equation which considers the deformation of the concrete floor beneath the base plate only, and this equation has already been proved to be inappropriate for initial stiffness predictions of the base-plate upright connection assembly (Sarawit 2003). Both, European specification (CEN 2009) and the Australian/New Zealand specification (SA 2012) recommend experimental tests to determine the initial stiffness of such base connections. Although the test setups proposed by these two specifications are similar, the Australian/New Zealand specification (SA 2012) provides additional clarifications, guidelines and recommendations for such tests.

Baldassino and Zandonini (2008), Gilbert and Rasmussen (2011), Godley *et al.* (1998), and others, have investigated the behavior of base-plate upright connections of regular steel storage pallet racks. Gilbert and Rasmussen (2011) also proposed a mechanical model to predict the initial stiffness of base plate assemblies of regular steel storage pallet racks. Their model incorporated the deformations of the upright and the concrete floor, however, it did not consider the deformation of the base-plate as well as the elongation of the associated anchor bolts. These studies show that the flexural behavior of base-plate upright connections assemblies is quite complex. The behavior can be characterized as a semi-rigid non-linear behavior, and the exact behavior depends very much on the configuration and composition of the base-plate upright connections. Thus, the observations and conclusions drawn from the investigations on regular unbraced pallet rack base plate assemblies may not be directly applicable to high-rise braced rack base plate assemblies. Besides, even though past studies considered the influence of axial loads on the behavior of base connections, influence of other parameters, namely, thickness of the base plate, the size of anchor bolts, the thickness of upright, and the height of bracket are yet to be studied. It must also be noted that, as far as the authors are aware, none of the published studies are directly related to the behavior of base-plate upright connection assemblies associated with the high-rise pallet racks.

An experimental investigation was recently conducted using nine groups of three identical base-plate upright connection assemblies associated with the high-rise steel storage racks. These experiments utilized an improved test arrangement based on the setup proposed by the European Standard EN 15512 (CEN 2009). The test program was designed to investigate the influence of axial load, thickness of the base plate, the size of anchor bolts, thickness of the upright, and the length of the bracket, on the flexural behavior of such connections. Since the pallet rack industry is not standardized, in practice, it is possible to have several combinations of base-plate upright connection assemblies having different geometric details and material properties. Obviously, a limited number of experimental tests cannot cover all the possible combinations of base connection configurations. The second part of the paper develops two analytical models for the initial stiffness of the connections under consideration. Since the base-plate and the anchor bolts play important roles, these mechanical models focus on the base-plate rotational stiffness including the influence of anchor bolts, and then combine with the concrete floor stiffness and the upright stiffness to obtain an overall rotational stiffness of the base-plate upright connection assembly. The analytical models results were compared with the experimental initial stiffness results.

2. Experimental investigation

2.1 The test specimens

As indicated in the previous section, a typical base-plate connection assembly of high-rise steel storage racks consists of a base-plate, anchored to the foundation using anchor bolts, and connected to an upright through a bolted-bracket or welded directly. The following parameters may influence the flexural behavior of base-plate upright connection assembly associated with the high-rise pallet racks; geometric properties, including the thickness, of the upright, thickness of the base-plate, the size and the location of the base-plate anchor bolt, the thickness of the bracket, the length of the bracket, as well as the axial load in the upright. The experimental investigation presented in this paper considered 9 groups of test specimens incorporating various influencing parameters associated with the base-plate upright connection assembly. Each group of tests consists of 3 identical tests. The Table 1 lists the variables under consideration. All test specimens used similar upright sections, having a profile as shown in Fig. 1, with an overall web height of 100 mm and the overall flange width of 94 mm. Except for specimen BP-8, whose upright was 2 mm thick, all other uprights were 3 mm thick (upright material thickness: 3 mm; Gross section area = 943.2 mm^2; Second moment of area about major axis = 1.24×10^6 mm^4; Second moment of area about minor axis = 0.924×10^6 mm^4; Experimental yield stress = 467.4 MPa; Axial load capacity = 440.9 kN). The base-plate used in this investigation was 240 mm in length and 110 mm in width. Except for specimen BP-6, whose base-plate thickness was 10 mm, all other base-plates were 15 mm thick (base-plate experimental yield stress = 263.2 MPa). Note that in good engineering construction practice, the size of the anchor bolts for use in such base connections is carefully selected to be compatible with the base plate thickness. In order mimic such practices, herein the specimens group BP-6 used M12 anchor bolts, whereas the remaining seven groups used M16 anchor bolts. The number indicates the nominal diameter of the anchor bolt. As highlighted in Fig. 1, the anchor bolts were located along the centroidal line of the upright, thus, forming a concentric connection. Except for group BP-9, specimens in which the upright was directly welded to the base-plate, in all other test specimens the upright was bolt connected to a bracket assembly fabricated from 4mm thick steel plates. In specimen groups BP-1 thru BP-8, the brackets were factory made to snug fit the upright, and the bracket and the upright were bolted together using #8 bolts (6 bolts in web and 2 bolts each in each flange). In specimens BP-1 to BP-8, the brackets were weld connected to the base-plate. The BP-9 tests provide benchmark results against which the performance of all other base-plate connection configurations may be compared. The brackets associated with the high-rise steel storage racks tend to be longer than that of the brackets used in regular pallet racks. This investigation considered 240 mm long brackets, except for specimen BP-7 which had a 165 mm long bracket. In these experiments, the upright length had to be selected with caution, such as to avoid premature local buckling and/or distortional buckling failure of the upright, and to reduce the shear deformation effects. Based on these considerations, 600 mm pieces of uprights were used in all of the test specimens. Specimens BP-1 thru BP-5 primarily consider the impact of axial loads, whereas, the specimens BP-6 thru BP-8 consider the influence of other geometric details on the behavior of base-plate upright connection assembly containing a bracket.

2.2 The test set-up

The tests under consideration intend to establish the flexural behavior (moment - rotation relationship) of base-plate upright connections, while the upright is under axial load. Such an axial load must be applied at the centroid of the upright cross-section in order to avoid the effects of load eccentricity. Past studies exist on similar tests on base connections associated with regular steel storage racks, and had prescribed the requirements for such a test setup. Castiglioni (2016) used two reaction frames and associated cables to apply the axial load and Firouzianhaji *et al.* (2014) adopted a four-bar linkage arrangement to apply the axial force. Godley *et al.* (1998) and Baldassino and Zandonini (2008) used two identical base-plate assemblies attached to a concrete block, which were then symmetrically loaded. In these studies the rotation of the concrete block was not prevented. Based on the review of past experiments on the base-plate upright connections the "Steel static storage

Table 1 The test specimens details

Specimen ID	Upright thickness (mm)	Base plate thickness (mm)	Base plate anchor bolt size	Bracket length (mm)	Axial load (kN)
BP-1	3	15	M16	240	50
BP-2	3	15	M16	240	10
BP-3	3	15	M16	240	25
BP-4	3	15	M16	240	75
BP-5	3	15	M16	240	125
BP-6	3	10	M12	240	50
BP-7	3	15	M16	165	50
BP-8	2	15	M16	240	25
BP-9	3	15	Upright welded directly to the base plate		50

*Note: In specimen groups BP-1 thru BP-8, the bracket and the upright were connected together using #8 bolts (6 bolts in web and 2 bolts each in each flange)

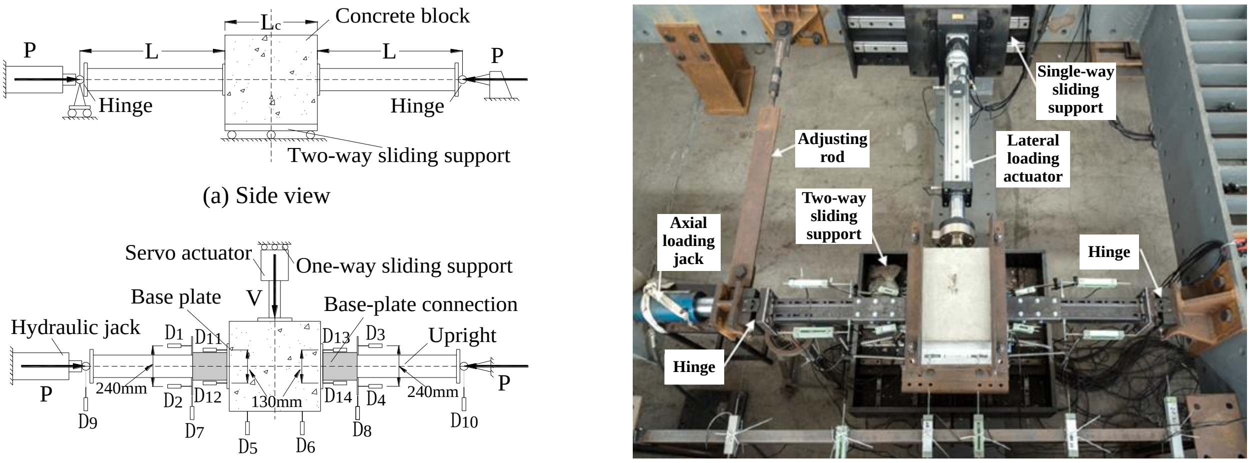

(a) Side view

(b) Plan view

(c) Photographic image

Fig. 2 Test set-up

systems—adjustable pallet racking systems— principles for structural design, EN 15512" published by European Committee for Standardization (CEN 2009), which was also adopted by the Australian/New Zealand, Steel storage racking Standards AS/NZS 4084 (SA 2012), requires that the rotation of the concrete block be restrained during the tests for the flexural behaviour of base-plate upright connections. Gilbert and Rasmussen (2011) used a test setup which could restrain the rotation of the concrete block, however, the frictional forces those may be introduced by the restraint (rigid plate - loading jack connection) was impossible to quantify, and thus, the actual moments applied on the test specimens may not be ascertained. Using the test setup for flexural behaviour of base-plate upright connection prescribed by the European Specification-EN 15512 (CEN 2009) and the Australian Standard- AS/NZS 4084 (SA 2012) as a guideline, this investigation establishes a refined test setup which could not only provide a perfect restraint of the rotation of the concrete block, and would also eliminate all possible frictional forces on the test specimen assembly.

Figs. 2(a) and (b) show the schematic of the test setup side view and the plan view, respectively, and Fig. 2(c) shows the photographic image of the test setup with a test specimen in place. In this setup, two identical test specimens were fastened to the opposite faces of a 400 mm cubic concrete block. The base-plate connections on either side were attached to the concrete block using two anchor bolts having diameter as shown in Table 1, spaced at 180 mm, and along the centreline of the base plate. The opposite ends of the two uprights of the test specimens were hinge supported through which an axial load was applied. During the test, first, one end of the upright was subjected to an axial load P, which was reacted at the opposite end. A lateral force V was then applied to the concrete block, using a 10 tonne actuator, which created the moments at the base-plate upright connections of the test specimens. In order to avoid shear forces in the V-actuator during application of axial force P, the V-actuator was mounted on a single-way sliding support (See Fig. 2(c)), which consists of a group of guide rails. The single-way sliding support allows the lateral loading V-actuator to move freely in sync with the concrete block, during the application of axial load P. This keeps the actuator load V perpendicular to the concrete surface during the whole test. In order to restrain the rotation of the concrete block about its vertical axis, the concrete block was mounted on a two-way sliding support system, which consists of two perpendicular groups of guide rails. These guide rails were manufactured with very high precision and they possess frictionless surfaces which allow the concrete block to move freely in the horizontal plane, without experiencing a rotation. During trial tests and during the actual tests, the horizontal movements of the concrete block were recorded using two displacement transducers, which confirmed zero rotation of the concrete block. The entire test setup, including the loading system, guide rails, and the reaction points, was situated within a specially designed closed loop rectangular reaction frame.

2.3 Displacement and strain measurements

The test setup used fourteen displacement transducers strategically mounted to monitor the movements of the test specimen and the concrete block and to obtain the moment-rotation relations. These displacement transducer locations are illustrated in Fig. 2(b). The transducers D1, D2, D3 and D4 were located just at the edge of the bracket of the base-plate upright assembly in order to capture the total rotation of the base joint, as is stipulated in AS 4084 specification (SA 2012). Note that for specimen BP-9, in which the upright was directly welded to the base plate, these LVDTs were mounted at 240 mm from the base plate, same distance used in other test specimens (The specimen BP-7 had 165 mm long bracket, and thus these LVDTs were mounted at 165 mm from the base plate). Due to the symmetrical arrangements of the test setup, the test specimen and the LVDTs, the transducer pairs (D1 & D3) and (D2 & D4) are expected to give the same readings. Fig. 3(a) shows representative load - displacement relations corresponding to these transducers. It is evident that the transducer pairs (D1 & D3) and (D2 & D4) experienced identical readings, confirming that both sides of the base

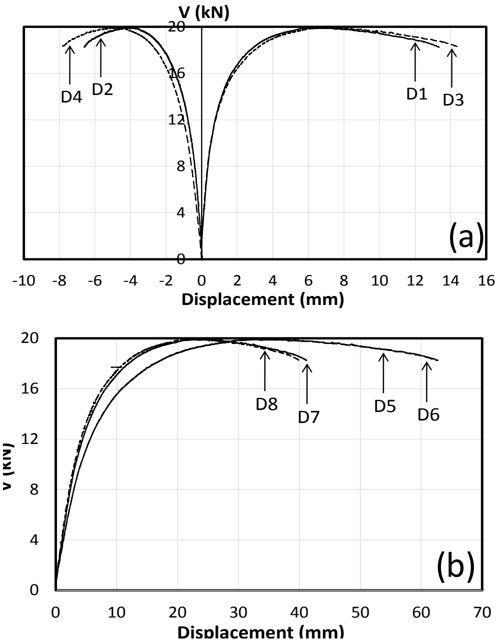

Fig. 3 Representative load - displacement responses (Test specimen BP-6-2)

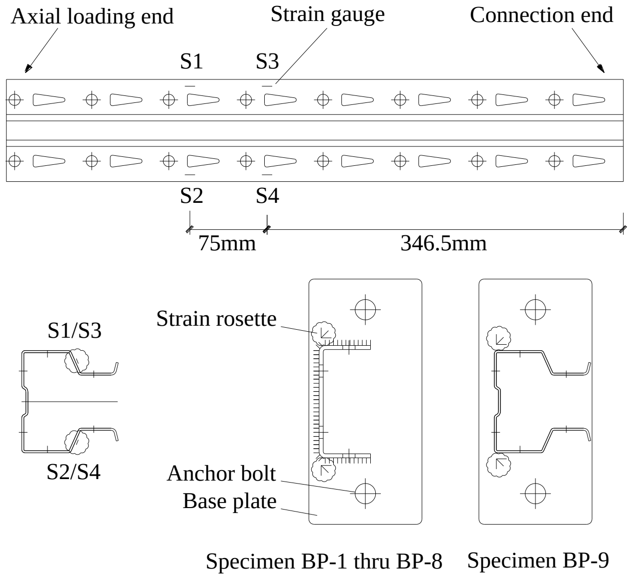

Fig. 4 Locations of strain gauges and strain rosettes

plate connections behaved in a symmetrical manner. Knowing the distance between these paired transducers (240 mm), the overall rotations of the left and the right sides of the base joints can be established as; $\theta_{Left} = (\delta_1 - \delta_2)/d_{12}$ and $\theta_{Right} = (\delta_3 - \delta_4)/d_{34}$, where, δ_i is the displacement recorded by transducer i , and $d_{ij} = d_{12} = d_{34} = 240$ mm is the distance between transducers i and j, respectively. Capitalizing on the symmetry, the rotation of the base-plate upright connection assembly can be taken as the average of the above two rotations (i.e., $\theta = [\theta_{Left}+\theta_{Right}]/2$).

As indicated previously, the moment was applied to the base-plate upright connection by applying a lateral force V to the concrete block. As a result, the concrete block experiences transverse displacements which were measured by LVDTs D5 and D6. Fig. 3(b) shows the load - displacements relations corresponding to D5 and D6 for specimen BP-6-2. The fact that D5 & D6 experience same displacements is the evidence that the concrete block do not rotate and that it experiences translations only. Therefore the lateral displacement of the concrete block Δ can be taken as $\Delta = (\delta_5 + \delta_6)/2$.

Fig. 3(b) also shows the lateral displacements at the end of the brackets, which were measured via transducers D7 and D8. The fact that the left side bracket and the right side bracket experienced identical amount of lateral displacements is a further proof that the test set up used in this investigation creates a truly symmetric loading of the test specimen. Assuming symmetry in loading, and counting the P-Δ moments, the total moment experienced by the base-plate upright connections corresponding to a transverse load V can be given as $M = (V/2) \times L + (P \times \Delta)$, where, V and P are the transverse and axial loads, respectively, L is the distance between the concrete base and the pin-support (See Fig. 2(a), L = 705 mm), and Δ is the applied transverse deflections at the base (concrete block). The base-plate itself may play a key role in the overall behavior of such connections. As shown in Fig. 2(b), the displacement transducers D11, D12, D13 and D14 were located at the upper surface of the base plate in order to capture the rotation of the base-plate itself. Unfortunately, due to obstructions such as bolts, etc., these four transducers were located at an angle. As a consequence, the recorded displacements were modified based on the geometric details in order to obtain the true displacements of the base-plate.

Based on these displacements the average rotation of the base plate can be obtained as; $\theta_{bp} = \{[(\delta_{11} - \delta_{12})/d_p] + [(\delta_{13} - \delta_{14})/d_p]\}/2$, where, δ_i is the modified displacement based on readings by transducer i, and d_p is the distance between these paired transducers, which is 130 mm (See Fig. 2(b)). The displacement transducers D9 and D10 were placed to measure the transverse deflection of the hinge ends, if any. These readings were zero, confirming zero transverse displacements at these ends.

Four strain gauges and two strain rosettes were attached to the left and to the right sides of the test specimen (total of 8 strain gauges and 4 strain rosettes) in order to monitor the test progress and to help understand the behavior of base-plate upright connections subjected to transverse and axial loads. The Fig. 4 shows the locations of such strain gauges and the strain rosettes on one side of the symmetric test specimen. The four strain gauges were attached to the upright flanges at a distance of 346.5 mm and 421.5 mm from the connection end of the upright. These strain gauge readings were used to guide application of the axial load through the centroid of the upright sections. As shown in Fig. 4, the strain rosettes were mounted on the surface of the base plate adjacent to the brackets in specimens BP-1 thru BP-8, and adjacent to the upright in specimen BP-9. These locations are thought to be of importance, since they may be the potential yielding locations of the base plate.

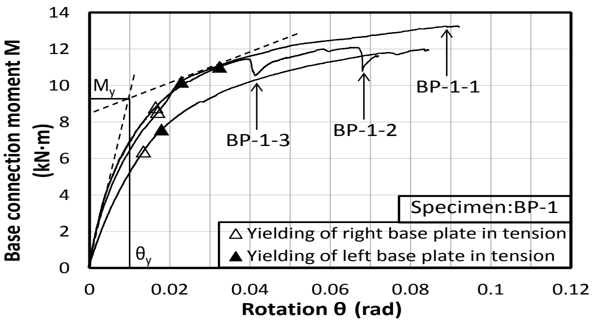

(a) Specimen BP-1

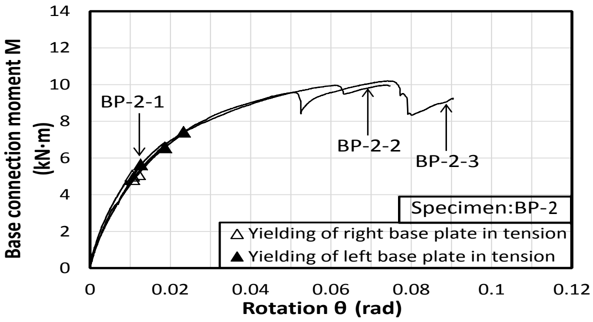

(b) Specimen BP-2

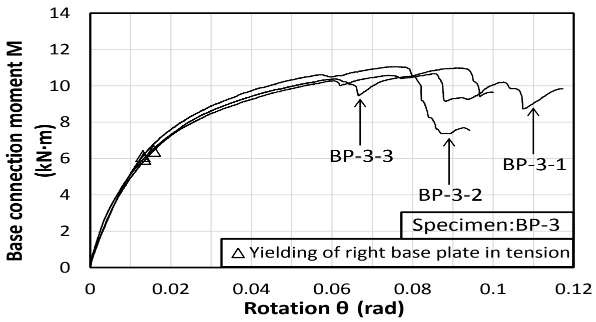

(c) Specimen BP-3

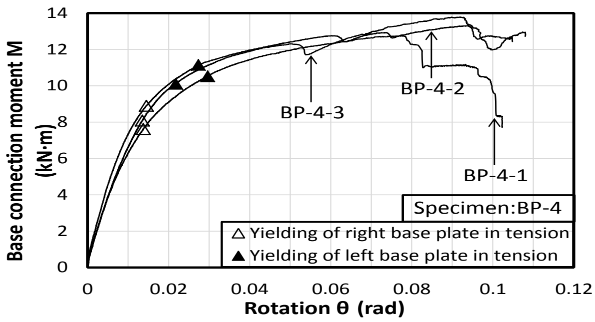

(d) Specimen BP-4

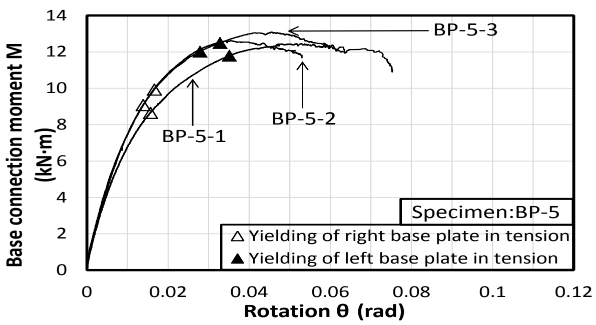

(e) Specimen BP-5

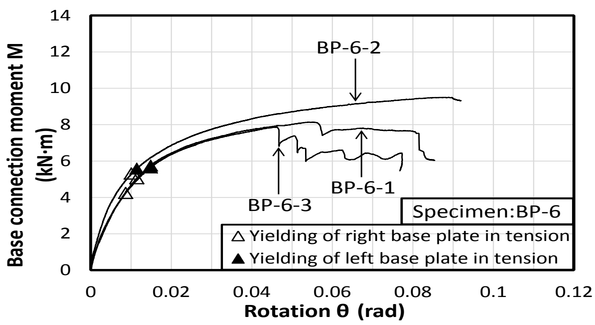

(f) Specimen BP-6

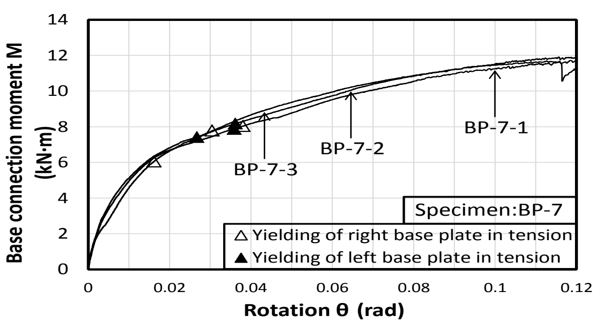

(g) Specimen BP-7

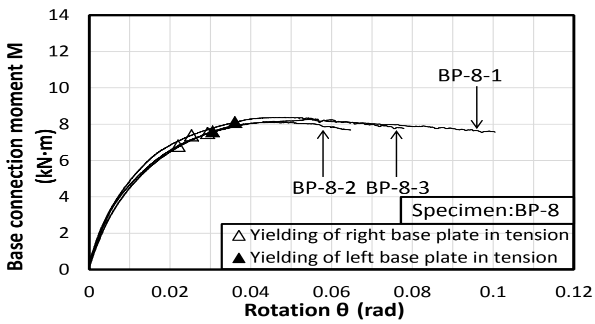

(h) Specimen BP-8

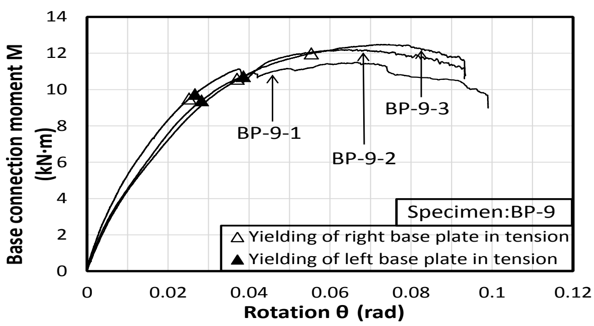

(i) Specimen BP-9

Fig. 5 Moment-rotation curves - Experimental results

Table 2 The experimental results

Specimen ID	Initial stiffness k_e (kN.m/rad)	Yield moment M_y (kN.m)	Rotation at M_y θ_y (rad)	Rotation at M_u θ_u (rad)	Moment capacity M_u (kN.m)	Failure mode
BP-1-1	893.5	9.2	0.010	0.041	11.6	Base-plate yielding
BP-1-2	977.4	8.7	0.009	0.036	11.2	Base-plate yielding[1]
BP-1-3	669.8	8.4	0.013	0.050	10.8	Base-plate yielding
BP-1	**846.9**	**8.8**	**0.011**	**0.042**	**11.2**	
BP-2-1	/	/	/	/	/	Incomplete test (ignored)
BP-2-2	626.0	7.2	0.011	0.046	9.3	Base-plate yielding
BP-2-3	609.1	7.1	0.011	0.044	9.3	Base-plate yielding
BP-2	**617.6**	**7.2**	**0.011**	**0.045**	**9.3**	
BP-3-1	651.8	7.4	0.011	0.045	9.6	Base-plate yielding[1]
BP-3-2	719.8	7.3	0.010	0.040	9.4	Base-plate yielding[1]
BP-3-3	611.0	8.1	0.013	0.053	10.5	Base-plate yielding[1]
BP-3	**660.9**	**7.6**	**0.011**	**0.046**	**9.8**	
BP-4-1	801.6	9.2	0.011	0.046	11.8	Base-plate yielding[3]
BP-4-2	922.4	9.5	0.010	0.041	12.0	Base-plate yielding
BP-4-3	806.7	9.7	0.012	0.048	12.2	Base-plate yielding[1]
BP-4	**843.6**	**9.5**	**0.011**	**0.045**	**12.0**	
BP-5-1	930.2	9.4	0.010	0.041	12.1	Base-plate yielding[3]
BP-5-2	909.8	10.6	0.012	0.047	12.2	Distortional buckling
BP-5-3	963.2	10.4	0.011	0.043	13.0	Distortional & local buckling
BP-5	**934.4**	**10.1**	**0.011**	**0.044**	**12.4**	
BP-6-1	634.4	5.9	0.009	0.037	7.6	Base-plate yielding
BP-6-2	786.6	6.0	0.008	0.030	7.7	Base-plate yielding
BP-6-3	739.3	5.5	0.007	0.030	7.1	Base-plate yielding[1]
BP-6	**720.1**	**5.8**	**0.008**	**0.032**	**7.5**	
BP-7-1	1008.0	5.3	0.005	0.021	6.9	Base-plate yielding
BP-7-2	917.9	5.4	0.006	0.023	6.9	Base-plate yielding
BP-7-3	789.6	5.9	0.007	0.030	7.6	Base-plate bending[3]
BP-7	**905.2**	**5.5**	**0.006**	**0.025**	**7.1**	
BP-8-1	643.2	6.2	0.010	0.039	8.0	Distortional buckling
BP-8-2	634.3	6.3	0.010	0.039	8.0	Distortional & local buckling
BP-8-3	677.7	6.4	0.009	0.038	8.1	Distortional & local buckling
BP-8	**651.7**	**6.3**	**0.010**	**0.039**	**8.0**	
BP-9-1	605.8	9.4	0.015	0.062	11.4	Base-plate yielding[2]
BP-9-2	674.5	9.5	0.014	0.057	12.1	Base-plate yielding[3]
BP-9-3	548.8	10.0	0.018	0.073	12.5	Base-plate yielding[3]
BP-9	**609.7**	**9.6**	**0.016**	**0.064**	**12.0**	

*Note: Base-plate yielding accompanied with [1]-Anchor bolt slippage; [2]-Local buckling of upright; [3]-Distortional buckling of upright

3. Test results and observations

3.1 Moment-rotation relations

The test program considered nine groups of test specimens, each consisting of three identical tests. As presented in the previous section, the base-plate upright connection moment at the base was established as $M = (V/2) \times L + (P \times \Delta)$ and the overall connection rotation was established as $\theta = [\theta_{Left}+\theta_{Right}]/2$. Fig. 5 shows the moment - rotation plots for each of the three identical test specimens.

It is evident that the moment-rotation relationships of such connections are highly nonlinear with a short linear range. Besides the geometric nonlinearity arising due to P-Δ effects, the local buckling and distortional buckling of upright, the anchor bolt slipping, and the base plate rotation and yielding may also cause nonlinear moment-rotation behaviour of the connection. In spite of the variability associated with such base-plate upright connection assemblies, three identical specimens exhibited consistent moment - rotation relationships. The initial slope of these plots is the experimental initial stiffness k_e of the base-plate upright connection assembly associated with braced high-rise steel storage racks. Table 2 lists the numerical values for the initial stiffness k_e of each test specimen. It also shows the average initial stiffness for each specimen group.

Since these types of connections consist of different components (base plate, bracket, upright) and the joining elements (anchor bolts, the bolts between upright and brackets, welds) and since the test setup may have minor misfit, the experimental initial stiffness values are expected to have some scatter. Analysis of 27 experimental initial stiffness values associated with nine groups of specimens indicated a largest relative standard deviation of 18.8% (Specimen group BP-1), whereas the average value of the relative standard deviation of initial stiffness associated with the nine groups of specimens was 7.7%.

Gilbert and Rasmussen (2011) indicated that the base-plate upright connection assemblies subjected to axial and transverse loads may not exhibit a clear peak moment. In the experimental results presented herein as well, as evident from Fig. 5, only the specimen groups BP-5, BP-8 and BP-9 exhibited clear peak moments. When no peak moment can be identified then a deformation limit may be used to identify the useful moment capacity of the connections. In this study, the deformation limit recommended by Gilbert and Rasmussen (2011), which is four times the yield deformation, was used as a criterion for determining the ultimate moment of base-plate upright connection assemblies. The yield moment and the associated yield deformation of the connection were taken as the values at the intersection of the initial slope and the post-yielding slope of 1/10th of the initial slope of the moment-rotation curve (ECCS 1986). The determination process of the yield rotation and the yield moment is illustrated in Fig. 5(a) using the experimental curve of Specimen BP-1-1. Table 2 summarizes the yield moment M_y, rotation associated with the yield moment θ_y, associated deformation limit θ_u (4 x yield rotation), and the moment capacity M_u for the 27 test specimens under consideration. As evident from Table 2, the moment capacities of identical test specimens were reasonably consistent with a largest relative standard deviation of 6.0% (Specimen group BP-3), whereas the average value of the relative standard deviation of moment capacities associated with the nine groups of specimens was 3.4%. The Table 2 also gives the average values for the yield moments, rotation associated with the yield moment, and the associated deformation limit rotations. While the scatter associated with the yield moments is comparable to that of the moment capacities, the rotation values exhibited considerable amount of scatter (largest relative standard deviation of 19.2% (Specimen group BP-7). It may be pointed out that the peak moments associated with the specimen groups BP-5, BP-8 and BP-9, which exhibited clear peak moments, were 1-3% higher than the deformation limit based moment capacities established for these specimen groups (See Table 2).

(a) Base plate yielding (BP-2)

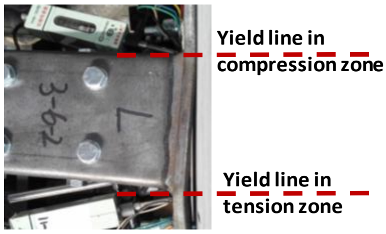

(b) Base plate yielding (BP-6)

(c) Upright distortional buckling (BP-5)

(d) Upright local buckling (BP-8)

(e) Upright local buckling (BP-9)

Fig. 6 Typical failure modes of base-plate upright connection assemblies

The initial yielding of the base-plate was monitored through two strain rosettes readings. Knowing the mechanical properties of the base-plate (not shown here) the yield state was established through von Mises stresses. The moments corresponding to the base plate yielding are also identified in Fig. 5 moment-rotation relations. The yielding of the right base plate and the yielding of the left base plate associated with a test specimen are distinguished in these graphs by hollow markers and solid markers, respectively. It can be observed that even though the test was symmetric the strain-rosettes based calculated yield moments associated with the left and right base plates were not the same, which may be due to loss of symmetry in the nonlinear range. Obviously, the moment-rotation curves become significantly nonlinear beyond the first yield of the base plate.

The base-plate upright connection assemblies of high-rise steel storage racks may fail by base-plate yielding in bending, or by the distortional and/or local buckling of uprights. The photographic images of representative failure modes observed during this test program are given in Fig. 6. Table 2 also summarizes the failure modes corresponding to each specimen under consideration. Majority of the connections failed due to base-plate yielding in bending and only a few of them failed by the distortional and local buckling of uprights. It is of interest to correlate that the specimens those exhibited distortional buckling and/or local buckling of uprights (specimen groups BP-5, BP-8 and BP-9) also exhibited clear peak moments. Other failure modes such as bracket failure, concrete block failure, and weld failure, were not noticed during these tests, however, anchor bolt slippage was observed in some of the test specimens, primarily at the end of the tests and well past the peak loading stages. It should be pointed out that due to the symmetrical and concentric location of the anchor bolts, the plastic hinge lines on the base-plate form parallel to the upright flanges. As illustrated in Fig. 6(b), the yield line in tension zone of the base plate, in general, appeared slightly outside the upright bracket tension flange, whereas, the compression yield line, in general, appeared adjacent to the upright bracket compression flange location.

3.2 Analysis of test results

3.2.1 Influence of axial loads

The Specimen Group BP-1 to Group BP-5 were intended to investigate the influence of axial compressive loads on the flexural behaviour of base-plate upright connection assemblies of high-rise steel storage racks. As shown in Table 1, these specimens were subjected to axial compressive loads ranging between 10 kN and 125 kN. Fig. 7 shows representative moment-rotation curves corresponding to these specimen groups. In general, increasing axial loads result in increasing initial flexural stiffness, as well as increasing moment capacities of base-plate upright connection assemblies. These observations are consistent with the observations made in previous studies by Baldassino and Zandonini (2008), and Gilbert and Rasmussen (2011). However, based on Fig. 7 and based on the values listed in Table 2, it appears that the initial stiffness does not proportionally increase with increasing axial compressive loads. Instead, the initial stiffness of specimens BP-2 and BP-3, on which the axial loads are lower than 50kN, are closer to each other, whereas, the initial stiffness of specimens BP-1, BP-4 and BP-5, which experienced more than or equal to 50 kN axial load, are also somewhat closer to each other. Considering that high-rise pallet racks are special light structures that carry heavy loads, the axial load in the upright may be always rather high, since the rack is often fully loaded. Therefore, it may be reasonable to state that the initial stiffness associated with high axial load may be of real use to designers, rather

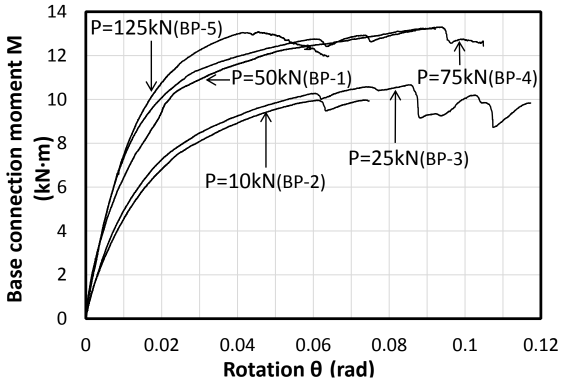

Fig. 7 Representative moment-rotation curves connections with axial loads

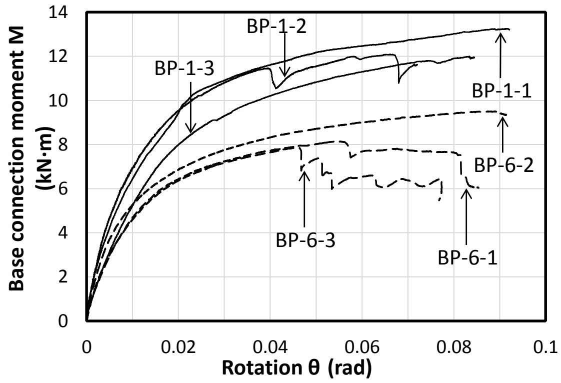

(a) Moment-rotation (M - θ) curves- Specimens BP-1 and BP-6

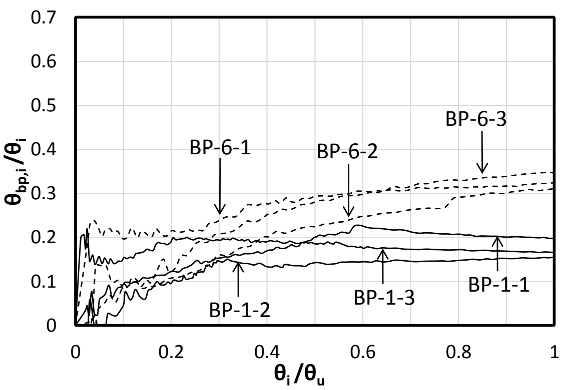

(b) Contributions of base plate component rotations to the overall rotations

Fig. 8 Impact of base-plate thickness on the flexural behavior of base connections than the initial stiffness of base-plate upright connections at low axial load.

The failure mode and ductility of base plate assemblies may also be influenced by the magnitude of the axial compressive load. The specimen groups those were subjected low compressive axial loads (BP-1 to BP-4) primarily failed by base-plate yielding in bending, whereas, BP-5, which was subjected to high axial load, failed by distortional buckling and local buckling of uprights. The ductility of these connections may be assessed by considering the rotations at yield moment and the rotations at moment capacity (see Table 2). Accordingly, even though the yield moments increased with increasing axial compressive loads, the corresponding yield rotations were constant (about 0.011 rad) regardless of the value of the axial load on the upright.

3.2.2 Influence of base-plate thickness

The impact of base-plate thickness (and the corresponding anchor bolt) on the moment-rotation behavior of the base connection can be investigated by comparing the results associated with specimen groups BP-1 and BP-6. As shown in Table 1, both groups of specimens were subjected to an axial load of 50 kN, however, the base-plate of BP-1 was 15 mm thick (M16 anchor bolts), whereas the base-plate of specimen group BP-6 was 10 mm thick (M12 anchor bolts). Fig. 8(a) shows the six moment-rotation curves for specimen groups BP-1 and BP-6. As shown in Table 2, on average, the initial stiffness of the BP-6 base connections was 15% less than that of BP-1, and the moment capacity of BP-6 is 33% less than that of specimen group BP-1. It may also be noted in Table 2 that rotation at yielding of specimens BP-1 is 0.011 rad, which is 38% higher than that of BP-6. Both specimens BP-1 and BP-6, however, eventually failed by base-plate yielding.

Since the base-plate anchor bolt assembly significantly influences the flexural behavior of such connections, the base-plate rotations were further investigated. Fig. 8(b) shows the variation of base-plate rotation as a percentage of the total rotation. In this figure, the vertical axis shows the ratio $\theta_{bp,i}/\theta_i$, where, $\theta_{bp,i}$ is the base-plate rotation at the loading level i (based on readings from displacement transducers D11, D12, D13 and D14), and θ_i is the total rotation at that corresponding loading level. For illustration convenience, the Fig. 8(b) uses a non-dimensional rotation of θ_i/θ_u as the horizontal axis. Herein, as shown in Table 2, θ_u is the rotation corresponding to the moment capacity associated with the connection. It could be observed from this graph that: (a) there is considerable immediate increase in the base-plate rotation, as soon as the connection is loaded with the lateral load V, which indicates that the base-plate experiences significant rotations from the instant the connection is subjected to external moments, (b) overall, the base-plate provides 20% of the connection rotations in specimens BP-1 which had 15 mm thick base plate and M16 anchor bolts, and (c) the base-plate rotations in specimens BP-6, which had 10 mm thick base plate and M12 anchor bolts, may be about 35% of the total rotations. It can be concluded from Fig. 8 that the thickness of the base-plate along with the size of the anchor bolt appear to significantly influence the stiffness and strength of high-rise steel storage rack base connections, and thus, their values must be selected prudently. The analytical models proposed in the next section, explicitly consider the contributions of the base-plate and the anchor bolt on the initial stiffness of the base-plate upright connection assembly associated with the high-rise steel storage racks.

3.2.3 Influence of the brackets

The influence of the bracket on the flexural behavior of base-plate upright connection assembly may be investigated using the results from specimens groups BP-1, BP-7, and BP-9. As indicated in Table 1, all four groups of specimens were subjected to an axial load of 50 kN, however, in specimen group BP-9 the upright was directly welded to the base-plate, thus, essentially BP-9 did not have a bracket. The BP-7 had a bracket length of 165 mm, whereas groups BP-1 had a bracket length of 240 mm. The Fig. 9 shows the representative moment-rotation relationships for these three groups of specimens, namely, BP-1, BP-7, and BP-9. As shown in Table 2, the initial stiffness of these three groups of specimens BP-1, BP-7, and BP-9 are 847, 905, and 610 kN.m/rad., respectively. It is no surprise that the specimens without a bracket, namely BP-9, exhibit the lowest initial stiffness, as the bracket enhances the initial stiffness of the base-plate upright connection assembly. The initial stiffness associated with specimen BP-7 was based on measured rotations at 165 mm, whereas the rest of the values were based on rotations measured at 240 mm. Thus, the initial stiffness values cannot be directly compared to each other, however, through basic mechanics, we estimated that the initial stiffness of BP-7 based on rotations at 240 mm would be about 754 kN.m/rad., which is 11% lower than the values we obtained for specimen group BP-1, which had a bracket length of 240 mm, indicating that longer bracket provides higher stiffness for the base-plate upright connection assembly. Also shown in Table 2, the moment capacities of these three groups of specimens BP-1, BP-7, and BP-9 are 11.2, 7.1, and 12 kN.m, respectively. Once again, since rotations were used to define the moment capacity of specimen BP-7, its moment capacity cannot be directly compared to the rest of the group, since the rotations were obtained at 165 mm. It is no surprise that the moment

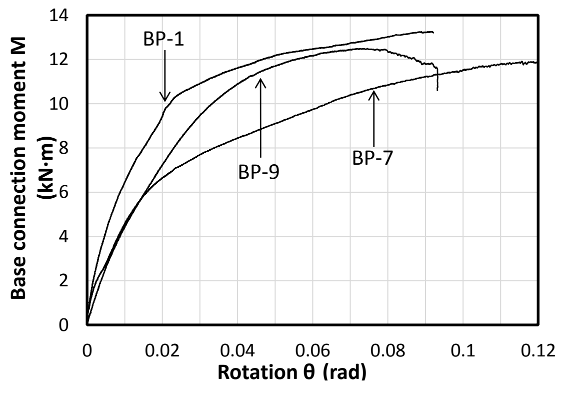

Fig. 9 Impact of bracket geometry on the moment-rotation relations (Specimen groups BP-1, BP-7, and BP-9)

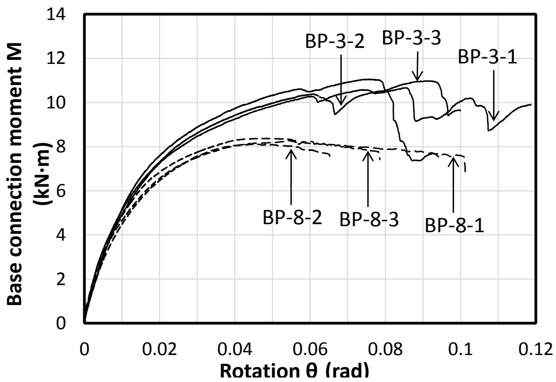

Fig. 10 Comparisons of moment-rotation curves between specimens BP-3 and BP-8

capacities of groups BP-1 and BP-9 were similar, since these specimens failed by the base-plate bending and yielding. Overall, the bracket is an important component in the base-plate upright connection assembly of high-rise steel pallet racks. The bracket transmits the moments and shear forces from the uprights to the base-plates and subsequently to the concrete floor. Nevertheless, we conclude that the influence of bracket on the overall behavior of the base-plate upright connection assembly is overshadowed by the dominant effects of the base-plate and of the upright.

3.2.4 Influence of the uprights

Specimens BP-3 and BP-8 can be used to investigate the influence of the thickness of the upright on the overall connection behavior, since BP-3 upright was 3 mm thick and BP-8 was 2 mm thick and both groups were subjected to the same value of axial load of 25 kN. The resulting moment-rotation curves are shown in Fig. 10. Even though the initial stiffness of these two groups of specimens are comparable (see Table 2), the moment capacity of specimen group BP-3, which has a thicker upright, was 22.5% higher than that of specimen group BP-8. It may be noted that the failure modes of these two specimen groups were different.

The specimen BP-8 failed due to the distortional and/or local buckling of uprights, whereas the specimen BP-3 failed by bending and yielding of the associated base-plate. The rotation capacity, reflected by the rotation at ultimate, of specimen group BP-3 is observed to be slightly better than the ductility of specimen group BP-8. As a general statement, the base-plate upright connections which failed in base-plate yielding exhibit larger ductility than those fail in buckling, such as upright local buckling, upright distortional buckling, etc.

4. Analytical models for the initial stiffness of base-plate upright connection with concentric anchor bolts

Herein, we develop two analytical models for the initial stiffness of base-plate upright connection assembly associated with high-rise steel storage racks, whose validity is verified through comparisons with the experimental results presented in Table 2. Gilbert and Rasmussen (2011) proposed an analytical model for the base connections associated with regular steel storage pallet racks. Their model, which utilized the component method, considered the elastic deformation of the concrete floor and the elastic deformation of the upright. Accordingly, Gilbert and Rasmussen (2011) established the initial rotational stiffness k_{cu} of the base connections as

$$k_{cu} = \frac{1}{\frac{1}{k_c} + \frac{1}{k_u}} \tag{1}$$

where, the rotational stiffness of concrete block was taken as $k_c = (7/25)bd^2E_c$, and where b and d are the width and depth of the upright section, respectively, and E_c represents the Young's modulus of the concrete floor. The above given concrete stiffness was, however, originally developed for regular racking structures by Sarawit (2003), which contained eccentric anchor bolts. Since the base-plate upright connections associated with the high-rise steel storage racks under consideration contain concentric anchor bolts, as per Sarawit (2003), the rotational stiffness of concrete block must be taken as $k_c = (9/25)bd^2E_c$. By considering a cantilever beam model, Gilbert and Rasmussen (2011) formulated the rotational stiffness of the upright as $k_u = (EI).\ (2L)/[(2L-a).a]$, where E and I are the Young's modulus and the second moment of area of the upright section, respectively, L is the length of the tested upright, and a is the location of the transducers where the base-plate upright assembly rotation was measured. In this investigation as well, we use the rotational stiffness of the upright derived by Gilbert and Rasmussen (2011). It should be emphasized, however, that Gilbert and Rasmussen (2011) model for initial stiffness, given by Eq. (1), considered the deformation of the concrete floor and the deformation of the upright only, and it did not include the deformations of the base-plate and the anchor bolts, which may be major participating components.

It was observed during the current experimental investigation, and as discussed earlier, the overall flexural behavior, including both the initial stiffness and the maximum bending moment, of the base-plate upright connection assembly associated with high-rise steel storage racks may be significantly influenced by the behavior of the base-plate. It is reminded that the behavior of base-plate is intertwined with the positions of the corresponding anchor bolts. The influence of base-plate in the connections associated with high-rise storage racks appears to be significant, which may be partly due to the fact that the anchor bolt position of high-rack base plate assemblies is different from that of normal-height racks, resulting in almost zero eccentricity between the bolt line and the centroid of the upright profile as compared with that of the normal-height racks. Even though the deformation pattern of the base-plate beneath the upright and the bracket may be complex in general, as observed during the tests, the base-plate assembly with concentric anchor bolt arrangement configuration currently under consideration leads to base-plate developing two yield lines parallel to the flanges of upright profile (See Fig. 6(b)), one on the tension side and the other one on the compression side of the connection. Essentially, the base-plate experiences significant flexural actions, which appear to be concentrated about the tensile and compression flanges of the brackets (when there is no bracket, consider the flanges of the upright, i.e., specimen BP-9). The following sections formulate the rotational stiffness of the base-plate anchor bolt assembly, founded on the above experimental observations.

For analysis purposes, the base-plate is divided into three different zones (see Fig. 11). Zone-I is the part of the base-plate which remains in contact with the concrete block throughout the test. The Zone-I is considered to extend up to the centerline of the compression flange of the bracket (when there is no bracket, consider the compression flange of the upright, i.e., specimen BP-9). The Zone-I of the base-plate primarily experiences bearing. The deformation of concrete due to this compression bearing is deemed to have been considered in the rotational stiffness of concrete k_c given previously. As observed during the experiments, the base-plate Zones-II & III are part of the base-plate that is considered to be experiencing uplift and is not considered to be in contact with the concrete block. However, this part is restrained by the anchor bolt. Assuming no contact of the tip, prying action need not be considered. As shown in Fig. 11, Zone-II is the part of the base-plate between the tension and the compression flanges of the bracket, whereas the Zone-III is the part of the base-plate that is held down by the tensile anchor bolt. This paper proposes two deformations models for Zones- II & III, one uses a rigid plate model, whereas the other uses an elastic plate model.

Rigid plate model: Herein, somewhat following the strategy used by the Eurocode 3—Design of steel structures (CEN 2005), we postulate that that the Zones-II & III of the base-plates rotate as two rigid bodies about the observed yield line locations (see Fig. 11(b)), i.e., compression and tension flange of the bracket (when there is no bracket, consider the flanges of the upright, i.e., specimen BP-9). The rotational resistance of the base plates at these locations is represented by a rotational springs having a stiffness of $k_\theta = E_{bp}.\ b_{bp}.(t_{bp})^2/12$, where E_{bp} is the modulus of elasticity of the base-plate, and b_{bp} and t_{bp} are the width and thickness of the base-plate, respectively (Jaspart and Vandegans 1998). The resistance provided by the anchor bolt is represented in this model as a linear spring having an axial stiffness of $k_a = E_a.\ A_a / L_a$, where, E_a is the modulus of elasticity of the anchor bolt, A_a is the effective area of the anchor bolt, and L_a is the effective length of anchor bolt in tension. According to Wald *et al.* (2008), the effective length of anchor bolts L_a may be taken as the sum of 8 times of the anchor bolt diameter, the thickness of gaskets, and half the thickness of the bolt head. Let us consider that the base-plate experiences a deflection of δ_1 at the tension flange location and a deflection of δ_2 at the tensile anchor bolt location. Consideration of moment equilibrium of Zone-III establishes the base-plate moment at tension flange location (Point T) as

$$M_T = (k_a \cdot \delta_2) \cdot d_2 \tag{2}$$

This moment can also be related to the rotational spring moment at location T as

$$M_T = k_\theta \cdot \left(\frac{\delta_1 - \delta_2}{d_2} + \frac{\delta_1}{d_1}\right) \tag{3}$$

The base-plate moment at the compression flange location C is

$$M_C = k_\theta \cdot \frac{\delta_1}{d_1} \tag{4}$$

Note that d_1 is the distance between compression and tension flanges of the bracket (when there is no bracket, consider the flanges of the upright, i.e., specimen BP-9) and d_2 is the distance between the tension flange and the tensile anchor bolt.

Consideration of the moment equilibrium of the Zones-II & III (together) about the compression flange location C gives

$$M_C - M + (k_a \cdot \delta_2) \cdot (d_1 + d_2) = 0 \tag{5}$$

Elimination of unrelated variables in the above equations and recognizing that the overall rotation of the base plate is (δ_1 / d_1) the base-plate anchor bolt assembly rotational stiffness k^R_{bp} can be derived as

$$k^R_{bp} = k_\theta \cdot \left(1 + \frac{k_a(d_1 + d_2)^2}{k_a d_2^2 + k_\theta}\right) \tag{6}$$

Note that the second part of the Eq. (6) is the rotational restraint provided by the anchor bolt. The Eq. (6) for the rotational stiffness of the base-plate and the tensile anchor bolts does not require any iterative process and thus could be easily used in engineering design calculations.

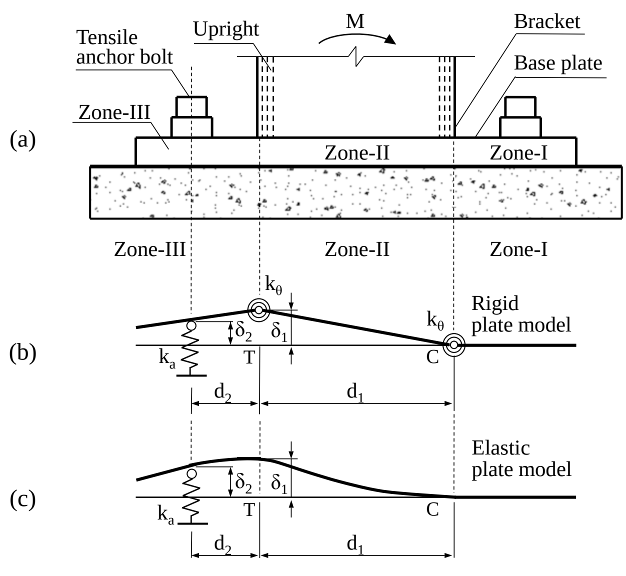

Fig. 11 Analytical models for the base plate

Elastic plate model: In this model, we postulate that that the Zones-II & III of the base-plates behave elastically during the early stages of loading, and experience one-way bending due to application of the moments on the upright (see Fig. 11(c)). The resistance provided by the anchor bolt is represented in this model as same as the rigid plate model, i.e., $k_a = E_a.\ A_a/L_a$. Assume that the base-plate experiences an elastic deflection of δ_1 at the tension flange location and an elastic deflection of δ_2 at the tensile anchor bolt location. From basic mechanics, the elastic deflection at the tension flange location δ_1 can be obtained as

$$\delta_1 = \frac{d_1^2}{3E_{bp}I_{bp}}\left[M - k_a\delta_2\left(d_1 + \frac{3}{2}d_2\right)\right] \tag{7}$$

where, M is the applied moment and E_{bp} is the modulus of elasticity of the base-plate, and $I_{bp} = b_{bp}.(t_{bp})^3/12$ is the second moment of area of the base-plate. Here, b_{bp} and t_{bp} are the width and thickness of the base-plate, respectively. Similarly, the elastic deflection at the tensile anchor bolt location δ_2 can be obtained as

$$\delta_2 = \frac{1}{3E_{bp}I_{bp}}\left[Md_1\left(d_1 + \frac{3}{2}d_2\right) - k_a\delta_2(d_1+d_2)^3\right] \tag{8}$$

Substituting δ_2 from Eq. (8) into Eq. (7), and recognizing that the overall rotation of the base plate is (δ_1/d_1) the base-plate rotational stiffness based on elastic plate model k^E_{bp} can be derived as

$$k^E_{bp} = \frac{3E_{bp}I_{bp}}{d_1}\left[\frac{1 + k_a(d_1+d_2)^3/3E_{bp}I_{bp}}{1 + k_a d_2^2\left(\frac{3}{4}d_1 + d_2\right)/3E_{bp}I_{bp}}\right] \tag{9}$$

The overall rotational stiffness of the base-plate upright connection assembly includes the participation of concrete floor, base plate, anchor bolts and the upright, and thus based on component method can be obtained as

$$k_{\text{connection}} = \frac{1}{\frac{1}{k_c} + \frac{1}{k_{bp}} + \frac{1}{k_u}} \tag{10}$$

Note that when considering the rigid body model, Eq. (6) must be used as base-plate stiffness k_{bp} in the above equation, and when considering the elastic model, Eq. (9) must be used as base-plate stiffness, and the resulting overall connection initial stiffness values have been identified in this paper as k^R and k^E, respectively. Above proposed analytical models for the initial stiffness of base-plate upright connection assembly were applied to the nine groups of specimens considered during the experimental phase. Table 3 shows the average experimental initial stiffness values for specimens group BP-1 thru BP-9, along with the predicted initial stiffness values using the two different mechanical models. The column (2) of Table 3 shows the average experimental initial stiffness values, which were extracted from Table 2. The column (3) shows the predicted initial stiffness values based on Gilbert and Rasmussen (2011) model given by Eq. (1), which does not include the stiffness of the base-plate and column (4) shows these predicted values as a ratio of the experimental results. Eq. (1) predicted initial stiffness values are consistently higher (21% to 87% higher) resulting on an average of 53% higher prediction. Column (5) gives the predicted initial stiffness values based on the rigid-plate analytical model derived herein, whereas, in column (6) these values had been compared with the corresponding experimental results. Four of the predicted values were less than the corresponding experimental results (lowest 12% less) and other five were higher than the corresponding experimental results (largest 33% higher). Overall, on average, the proposed rigid plate model gives about 8% overestimation.

The initial stiffness values based on elastic plate model for the base-plate are listed column (7), and these values were compared with the corresponding experimental results in column (8). Six of the elastic plate analytical model based values are less than the corresponding experimental initial stiffness values. The elastic model predictions give lower bound solutions resulting in 6% less average estimates of the initial stiffness, with a standard deviation of

Table 3 Comparisons of the initial stiffness values: Experimental versus predicted values

Specimen ID	Experimental k_e (kN · m/rad)	k_{cu} (kN · m/rad)	k_{cu}/k_e	k^R (kN · m/rad)	k^R/k_e	k^E (kN · m/rad)	k^E/k_e
(1)	**(2)**	**(3)**	**(4)**	**(5)**	**(6)**	**(7)**	**(8)**
BP-1	846.9	1138.8	1.345	823.2	0.972	746.1	0.881
BP-2	617.6	1138.8	1.844	823.2	1.333	746.1	1.208
BP-3	660.9	1138.8	1.723	823.2	1.246	746.1	1.129
BP-4	843.6	1138.8	1.350	823.2	0.976	746.1	0.884
BP-5	934.4	1138.8	1.219	823.2	0.881	746.1	0.798
BP-6	720.1	1138.8	1.581	710.2	0.986	440.7	0.612
BP-7	905.2	1495.1	1.652	994.5	1.097	884.1	0.977
BP-8	651.7	791.3	1.214	624.9	0.959	579.4	0.889
BP-9	609.7	1138.8	1.868	790.9	1.297	708.7	1.162
		Maximum	**1.868**		**1.333**		**1.208**
		Minimum	**1.214**		**0.881**		**0.612**
		Average	**1.533**		**1.083**		**0.949**
		Standard deviation	**0.258**		**0.167**		**0.192**

about 19%. As explained earlier, the initial stiffness of base connections associated with high axial load may be of real use to the rack designers, thus the proposed models did not explicitly consider the impact of axial loads on the initial stiffness of base-plate upright connection assembly. The analytical results confirm the fact that the base plate and anchor bolt assembly greatly influences the overall rotational stiffness of the base-plate upright connection assembly and it is important to recognize its stiffness in the analysis and design of base connections for high-rise steel storage racks. These results are further illustrated in Fig. 12, where the horizontal axis shows the experimental initial stiffness values, and the vertical axis shows the analytical model predicted values. It is evident that both proposed analytical models give reasonably good prediction of the rotational stiffness of the base-plate upright connection assembly under consideration. Data analysis indicated that one can say with 90% confidence that the rigid plate model predicted initial stiffness values are between 99% and 120% of the experimental results, whereas the elastic plate model predicted values are between 84% and 108% of the experimental results.

5. A parametric study for the initial stiffness of base-plate upright connection (concentric anchor bolts)

In order to further understand the behavior of the base-plate upright connection with concentric anchor bolts and to provide further guidance for the rack designers, this section discusses the parametric study results for the initial stiffness of such connections based on the rigid-plate model and the elastic-plate model proposed in the previous section. Influencing parameters such as the base-plate thickness, the anchor bolt diameter, the anchor bolt locations and the upright thickness were considered in this investigation.

In an attempt to understand the interplay of concrete block, base-plate and the upright on the overall rotational stiffness of the base-plate upright connection assembly, the $k_{connection}$ given in equation (10) can be rewritten as

$$k_{\text{connection}} = \frac{k_c . k_{bp} . k_u}{[k_c . k_{bp} + k_c . k_u + k_{bp} . k_u]} \tag{11}$$

It can now be easily visualized that (a) the overall rotational stiffness $k_{connection}$ will always be less than the lowest stiffness among k_c, k_{bp}, and k_u. The stiffness of the concrete block used in the experiments, and assumed in the parametric study, was established as k_c = 10152 kN.m/rad., which is the largest value (many times more than k_{bp}, and k_u), and thus the $k_{connection}$ will always be less than the lower stiffness between k_{bp}, and k_u (b) any enhancement to the lowest stiffness element will provide considerable enhancement in the overall rotational stiffness, until its stiffness value approaches the higher stiffness value.

5.1 Influence of the base-plate thickness

Fig. 13 graphically demonstrates the influence of the base-plate thickness on k_{bp} and on the overall initial stiffness of such connections. Potential base-plate thickness range for such connections of 4 mm to 18 mm is under consideration. This part of the parametric study used 3 mm thick upright, and M16 anchor bolts located at 37 mm from the center line of the bracket flanges. Fig. 13 shows that the trends in initial stiffness values derived from the rigid-plate model and the elastic-plate model are somewhat similar to each other. The initial stiffness values derived from rigid-plate model remain consistently higher than the values derived from the elastic-plate model, which agrees with the concept that the rigid-plate model, in which the base-plate rotations were concentrated at bracket flange locations thus giving upper bound solutions. The overall stiffness is sensitive to changes in base-plate thickness as long as $k_{bp} < k_u$ (Rigid plate model: approximately up to 10mm thick base plate). In this range, doubling the thickness of the base-plate increases the overall stiffness of the base connection by at least 3 times. When $k_{bp} > k_u$, as expected, the change in overall stiffness is marginal. Therefore, we recommend to the rack designers and manufacturers that increasing the thickness of base-plates is an efficient option to increase the overall initial stiffness of base-plate assemblies, provided the stiffness of the base-plate

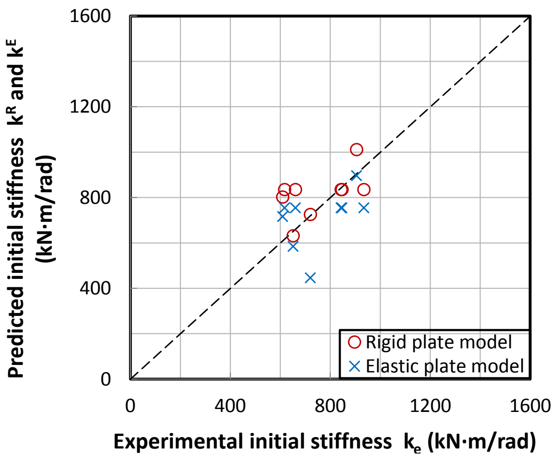

Fig. 12 Analytical models predicted initial stiffness values versus experimental results

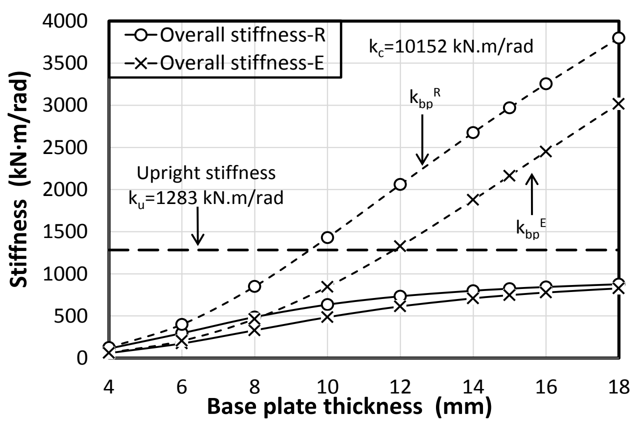

Fig. 13 Influence of base plate thickness on the initial stiffness

assembly is less than the stiffness of the upright.

5.2 Influence of the anchor bolt diameter

It can be seen from Eqs. (6) and (9) that the stiffness of the base-plate anchor bolt assembly depends on the stiffness of the anchor bolt k_a, i.e., the diameter of the anchor bolts. This part of the parametric study investigates the influence of anchor bolt diameter (bolt size range M8 to M18; the number indicates the nominal diameter of the anchor bolt) on the stiffness of the base-plate anchor bolt assembly, and on the overall stiffness of such connections. The calculations considered three base-plate thicknesses namely, 6 mm, 12 mm and 18 mm and explicitly show for rigid-plate model only. Consistent with the experimental specimens the study used a 3 mm thick upright with anchor bolts set at a distance of 37 mm from the center line of the bracket flanges. It is evident from Fig. 14 that anchor bolt does influence the stiffness of the base-plate anchor bolt assembly, however, its contribution depends on the relative stiffness of the base- plate. In thin base-plate (e.g., 6 mm base-plate) distances dictate the base-plate stiffness k_{bp}, whereas, the influence of anchor bolt stiffness becomes noticeable in thicker base-plates. For example, use of M16 in 18mm base-plate increases k_{bp} value by 72% compared to the use of M8 anchor bolt. Unfortunately, in this part of the study the base-plate stiffness values for 18 mm and 12 mm plates with M8 to M18 bolts are higher than that of the upright, and thus do not cause any noticeable change in the overall stiffness values of the base-plate upright connection assembly.

Furthermore, the influence of anchor bolt size on the 6 mm base-plate was minimal, which translated into minimal change in the overall rotational stiffness of the connection. Nevertheless, we recommend to the rack designers and manufacturers that increasing the anchor bolt size is also a viable option to increase the base-plate assembly stiffness in connections having thicker base-plates.

5.3 Influence of the anchor bolt location

As described in the analytical models proposed in the previous section, the quantity d_1 represents the distance between the center lines of the tension/compression bracket flanges and is determined by the upright depth and the bracket thickness, and d_2 is the distance between the tensile anchor bolt and the center line of the tensile bracket flange. This part of the parametric study used 3 mm thick upright and 15 mm base-plate M16 anchor bolts assembly, with variable quantity d_2. The Fig. 15 illustrates the influence of anchor bolt location d_2 (shown in the horizontal axis as a non-dimensional parameter d_2/d_1 from 0.2 to 1.2) on the stiffness of the base-plate anchor bolt assembly and on the overall stiffness of the of base-plate upright connections. Generally speaking, the base-plate anchor bolt assembly stiffness decreases as anchor bolt location distance d_2 increases. This decrease in the initial stiffness is more pronounced in the results based on the elastic-plate model, as compared with the rigid-plate model, which is due to the fact that the elastic-plate model incorporated the flexural deflections of the base-plate component resulting in larger deflections for increasing values of d_2. As evident from Fig. 15, the reduction in overall stiffness of the base-plate upright connection becomes significant, if and only if the base-plate stiffness falls below the upright stiffness. According to elastic-plate model the reduction in stiffness of the connections under consideration would have been marginal up to anchor bolt location $d_2 < 0.6\ d_1$, which is about 60 mm, whereas the experiments used 37 mm. Based on this part of the investigation, it is recommended that the anchor bolts be located as close as possible to the bracket flanges in order to achieve higher initial rotational stiffness of base-plate connections.

5.4 Influence of the upright thickness

This part of the parametric study investigated the influence of the upright thickness on the initial stiffness of base-plate upright connections. Even though the upright thickness is usually determined by the required resistance of the upright and could not be arbitrarily changed when designing the column bases, the rack designers will benefit by knowing the extent of the influence the upright thickness may have on the initial stiffness of such connections. The Fig. 16 shows the influence of the upright thickness on the overall initial stiffness of base-plate upright connections having different base plate thicknesses, established based on

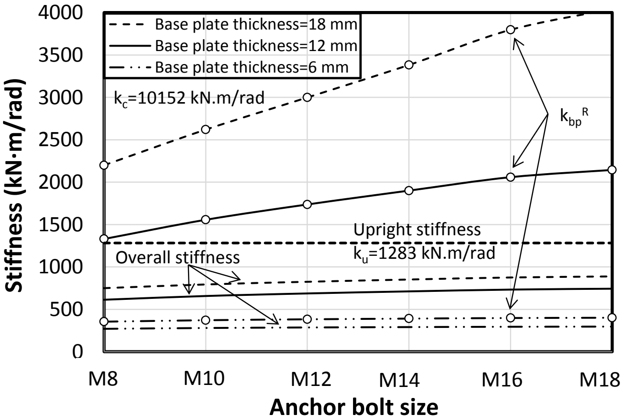

Fig. 14 Influence of anchor bolt diameter on the stiffness

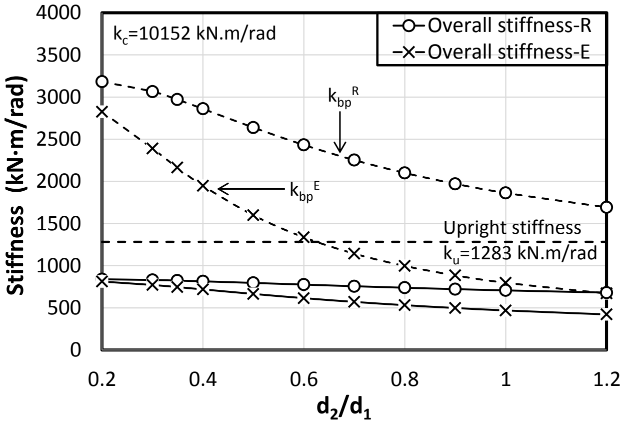

Fig. 15 Influence of the anchor bolt location on the initial stiffness

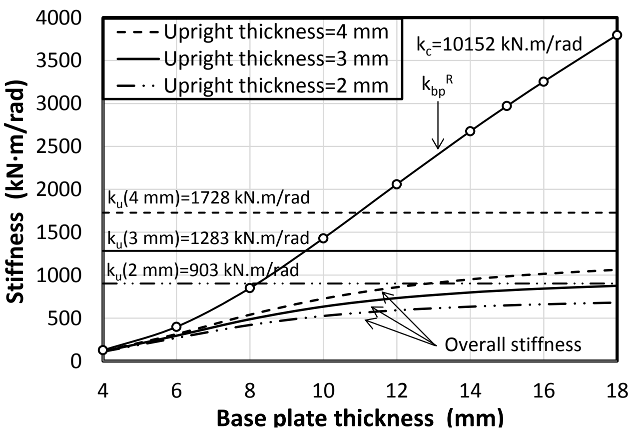

Fig. 16 Influence of upright thickness on the initial stiffness

rigid-plate model only. Though not shown herein, the elastic-plate model exhibited similar results. In this part of the parametric study, even though the base-plate thicknesses were changed, M16 anchor bolts were assumed, and the anchor bolts were assumed to be located at a distance of 37 mm from the center line of the bracket flanges. As highlighted earlier, the overall stiffness is sensitive to changes in base-plate thickness as long as $k_{bp} < k_u$, which is evident in Fig. 16. From this part of the investigation, as far as the efficient maximization of overall rotational stiffness is concerned, 2 mm upright may use 8 mm thick base-plate, 3 mm upright may use about 10 mm thick base-plate and 4 mm upright may use 12 mm base-plate. As indicated earlier, the rack engineering practice may require larger size anchor bolts with thicker base-plate to resist largest lateral loads and to prevent uplift, which can further enhance the overall rotational stiffness.

6. Conclusions

A review of research literature on pallet racks indicated that the flexural behavior of high-rise rack base-plate upright connection assembly is not readily available. Therefore, this investigation experimentally established the flexural behavior of concentrically anchor bolted connections using nine groups of three identical test specimens. This study led to development of an improved test setup, which could not only completely restrain the rotation of concrete block, and thus, perfectly meeting the requirements of the rack specifications, but also would eliminate the effects of the frictional forces on the moment-rotation curves. The experiments considered the influence of axial load, thickness of base plate, size of the anchor bolt, length of bracket and the thickness of uprights on the initial rotational stiffness, and the moment capacity of the base connections for high-rise steel storage racks. The results show that increasing axial load on the upright results in higher flexural stiffness and moment capacity of the base connections. The enhancement of the base-plate assembly components, namely base-plate thickness and anchor bolt-size, causes significant changes in the initial stiffness associated with the base connections under consideration. Limited experiments indicated that the thickness of the upright causes marginal changes in the initial stiffness. The eventual failure mode determines the rotational capacity associated with such connections and, as a general statement, base-plate yielding failure exhibits larger rotations than those fail in buckling, such as upright local buckling, upright distortional buckling, etc. Two analytical models, namely, rigid-plate model and elastic-plate model, for the base-plate upright connections associated with the high-rise rack structures were also developed in this paper, in order to understand the interplay of concrete block, base-plate and the upright on the overall rotational stiffness of the base-plate upright connection assembly and to facilitate prediction of overall rotational stiffness of such connections without resorting to experiments. It was shown that the analytical model provides reasonable estimation of initial stiffness values observed during the experimental investigation. Furthermore, the parametric studies show that (a) increasing the thickness of base-plates is an efficient option to increase the overall initial stiffness of base-plate assemblies, provided the stiffness of the base-plate assembly is less than the stiffness of the upright. (b) increasing the anchor bolt size is also a viable option to increase the base-plate assembly stiffness in connections having thicker base-plates (c) the proposed analytical models provide a means for efficient maximization of overall rotational stiffness of concentrically anchor bolted high-rise rack base-plate upright connections.

Acknowledgments

The work presented in this paper was funded by the National Key R&D Program of China (No. 2016YFC0701603). The authors would like to thank WAP Logistics Equipment (Shanghai) Co., Ltd for providing all the test specimens in this experimental program.

References

Baldassino, N. and Bernuzzi, C. (2000), “Analysis and behaviour of steel storage pallet racks”, *Thin-Wall. Struct.*, **37**(4), 277-304. https://doi.org/10.1016/S0263-8231(00)00021-5

Baldassino, N. and Zandonini, R. (2008), “Performance of base-plate connections of steel storage pallet racks”, *Proceedings of 5th International Conference on Coupled Instabilities in Metal Structures* (*CIMS2008*), Gregory J. Hancock Symposium, Sydney, Australia.

Beale, R.G. and Godley, M.H.R. (2001), “Problems arising with pallet rack semi-rigid baseplates”, *Proceedings of the 1st International Conference on Steel and Composite Structures*, Busan, Korea, pp. 699-706.

Bernuzzi, C., Gobetti, A., Gabbianelli, G. and Simoncelli, M. (2015), “Simplified approaches to design medium-rise unbraced steel storage pallet racks. I: Elastic buckling analysis”, *J. Struct. Eng.*, **141**(11), 04015036. https://doi.org/10.1061/(ASCE)ST.1943-541X.0001271

Castiglioni, C.A. (2016), *Seismic Behavior of Steel Storage Pallet Racking Systems*, (First Ed.), Springer International Publishing, Berlin, Germany.

ECCS N°45 (1986), Recommended Testing Procedure For Assessing the Behaviour of Structural Steel Elements under Cyclic Loads, Technical Committee 1 – Structural Safety and Loadings Technical Working Group 1.3 – Seismic Design.

El Kadi, B., Cosgun, C., Mangir, A. and Kiymaz, G. (2017), "Strength upgrading of steel storage rack frames in the down-aisle direction", *Steel Compos. Struct., Int. J.*, **23**(2), 43-152. https://doi.org/10.12989/scs.2017.23.2.143

EN 15512 (2009), Steel static storage systems—adjustable pallet racking systems—principles for structural design, European Committee for Standardization (CEN), Brussels, Belgium.

Eurocode (2005), Design of steel structures. Part 1.8: Design of joints, European Committee for Standardization (CEN), Brussels, Belgium.

Firouzianhaji, A., Saleh, A. and Samali, B. (2014), "Non-linear finite element analysis of base plate connections used in industrial pallet racking structures", *Proceedings of Australasian Structural Engineering Conference* (*ASEC*), Auckland, New Zealand.

Gilbert, B.P. and Rasmussen, K.J.R. (2011), "Determination of the base plate stiffness and strength of steel storage racks", *J. Constr. Steel Res.*, **67**(6), 1031-1041. https://doi.org/10.1016/j.jcsr.2011.01.006

Godley, M.H.R., Beale, R.G. and Feng, X. (1998), "Rotational stiffnesses of semi-rigid baseplates", *Proceedings of 14th International Specialty Conference on Cold-formed Steel Structures*, St. Louis, MO, USA.

Jacobsen, E. and Tremblay, R. (2017), "Shake-table testing and numerical modelling of inelastic seismic response of semi-rigid cold-formed rack moment frames", *Thin-Wall. Struct.*, **119**, 190-210. https://doi.org/10.1016/j.tws.2017.05.024

Jaspart, J.P. and Vandegans, D. (1998), "Application of the component method to column bases", *J. Constr. Steel Res.*, **48**(2-3), 89-106. https://doi.org/10.1016/S0143-974X(98)90196-1

Kadi, B.E. and Kiymaz, G. (2015), "Behavior and design of perforated steel storage rack columns under axial compression", *Steel Compos. Struct., Int. J.*, **18**(5), 1259-1277. https://doi.org/10.12989/scs.2015.18.5.1259

Kilar, V., Petrovčič, S., Koren, D. and Silih, S. (2011), "Seismic analysis of an asymmetric fixed base and base-isolated high-rack steel structure", *Eng. Struct.*, **33**(12), 3471-3482. https://doi.org/10.1016/j.engstruct.2011.07.010

Petrone, F., Higgins, P.S., Bissonnette, N.P. and Kanvinde, A.M. (2016), "The cross-aisle seismic performance of storage rack base connections", *J. Constr. Steel Res.*, **122**, 520-531. https://doi.org/10.1016/j.jcsr.2016.04.014

RMI (2008), Specification for the design, testing and utilization of industrial steel storage racks, Rack Manufacturers Institute; Charlotte, NC, USA.

SA (2012), AS/NZS 4084 Steel storage racking, Standards Australia /Standards New Zealand, Sydney, Australia.

Sarawit, A.T. (2003), "Cold-formed steel frame and beam column design", Ph.D. Dissertation; Cornell University, Ithaca, NY, USA.

Shah, S.N.R., Sulong, N.R., Jumaat, M.Z. and Shariati, M. (2016), "State-of-the-art review on the design and performance of steel pallet rack connections", *Eng. Fail. Anal.*, **66**, 240-258. https://doi.org/10.1016/j.engfailanal.2016.04.017

Silvestre, N. and Camotim, D. (2004), "Distortional buckling formulae for cold-formed steel rack-section members", *Steel Compos. Struct., Int. J.*, **4**(1), 49-75. https://doi.org/10.12989/scs.2004.4.1.049

Valipour, H.R. and Bradford, M.A (2013), "Nonlinear P-Δ analysis of steel frames with semi-rigid connections", *Steel Compos. Struct., Int. J.*, **14**(1), 1-20. https://doi.org/10.12989/scs.2013.14.1.001

Wald, F., Sokil, Z. and Jaspart, J.P. (2008), "Base plate in bending and anchor bolts in tension", *Heron*, **14**(1), 1-20.

BU